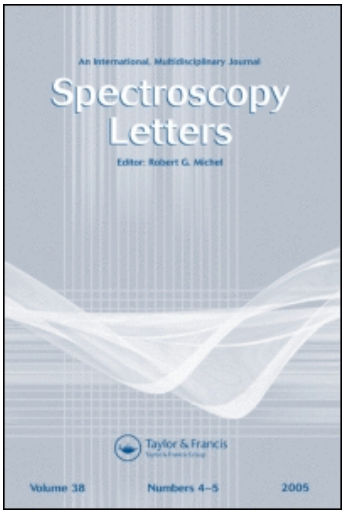

Spectroscopy Letters
Publication details, including instructions for authors and subscription information:
http://www.informaworld.com/smpp/title~content=t713597299

in situ FTIR Spectroscopic Characterization of Electroactive Species

Monika Datta[a]; Arunabha Datta[a]
[a] Department of Chemistry, University of California, Santa Barbara, California

To cite this Article Datta, Monika and Datta, Arunabha(1986) 'in situ FTIR Spectroscopic Characterization of Electroactive Species', Spectroscopy Letters, 19: 9, 993 — 1037
To link to this Article: DOI: 10.1080/00387018608069304
URL: http://dx.doi.org/10.1080/00387018608069304

SPECTROSCOPY LETTERS, 19(9), 993-1037 (1986)

IN SITU FTIR SPECTROSCOPIC CHARACTERIZATION OF ELECTROACTIVE SPECIES

Monika Datta and Arunabha Datta
Department of Chemistry
University of California
Santa Barbara
California 93106

ABSTRACT

A spectroelectrochemical technique based on the Fourier Transform Infrared Reflection Absorption Spectroscopic (FTIR-RAS) method is described, whereby high resolution in situ vibrational spectra of electrogenerated reaction intermediates (including radicals) and species adsorbed on electrode surfaces are obtained. Theoretical and experimental aspects of the method in a single reflection mode are discussed. Details of the cell design and the optimization of the operational parameters for running the FT-IR spectrometer in the RAS mode are also described. Apart from the potential of this technique to identify adsorbed species through their vibrational spectra, it can also be used to determine the orientation of the adsorbed species on the electrode surface by making use of surface selection rules. Using this

0038-7010/86/1909-0993$3.50/0

technique, it has been possible to record the spectra of molecules adsorbed from aqueous and non aqueous media on metal and carbon electrodes. It has been possible to distinguish the vibrational spectra of adsorbed molecules from those in the bulk. Various systems covering a wide range of molecules have been studied and the potential of the technique as a method for the characterization of the electrode-electrolyte interface has been demonstrated.

INTRODUCTION

The determination of electrochemical reaction pathways essentially involves the detection, identification and kinetic monitoring of intermediates and/or products generated either at the electrode surface or in the adjacent solution. In particular the formation of molecular ions like anion and cation radicals as short-lived intermediate species, distinguishes a great many chemical reaction. While voltametric measurements can provide information concerning surface coverage and reaction rates, these methods are limited to the extent that the electrical quantity measured (potential, current or charge) corresponds to the cumulative action of the individual step (1). It is essential therefore to have complementary in situ physicochemical methods that can provide further detailed information concerning the chemical identity and kinetic behavior of adsorbed species, their interaction with the substrate surface and the structure and constitution of the electrical double layer. Modern physical methods of surface characterization such as Low Energy Electron Diffraction, Field Electron and Ion Emission Microscopy, X-ray Photoelectron and Auger Electron Spectroscopy have enabled the details of molecular processes on solid surfaces to be studied with microscopic resolution. Such methods however, are not applicable to studies of the surface of a metal or semiconductor electrode immersed in a liquid electrolyte.

For the in situ characterization of an electrode surface, optical spectroscopy is one of the most versatile physicochemical methods. Electron absorption spectroscopy for instance, has been widely used owing to the high sensitivity and large extinction coefficients and since it can be coupled to electrochemistry in both transmission and reflection modes. However, the utility of this technique, for the purpose of identification, is limited by the low information content of UV-Visible spectra.

Several attempts have been made to couple vibrational spectroscopy with electrochemistry. The motivation for this is the greater degree of molecular specificity and sensitivity to subtle environmental factors inherent in vibrational spectroscopy. However, the use of Raman spectroscopy is mainly restricted to species which show resonance or surface enhancement, owing to the lack of sufficient sensitivity in normal Raman scattering. Moreover, the limited choice and availability of exciting laser lines, imposes a further restriction on the use of Raman spectroscopy. In addition, for a molecule of low symmetry, the IR absorption will, in general be more detailed and will provide more information on the molecular vibrational modes than the corresponding resonance Raman spectrum (2).

It is not suprising therefore, that in recent years, infrared spectroscopy has been increasingly used for the study of electrochemical processes (3,4,5).

The purpose of this paper is to provide a background of the theory and technique required for the use of infrared specular reflection spectroscopy, in a single reflection mode, using an FT-IR spectrometer and to demonstrate the utility of this technique for the characterization of electrogenerated species at the electrode surface and/or in the solution.

SPECULAR REFLECTION OF ELECTROMAGNETIC RADIATION

The specular reflectivity of a substrate depends on its optical constants (n,k), angle of incidence (θ), polarization of incident radiation and the conductivity of the substrate (σ). The reflectivity of an interface is given by the expression

$$R_{12} = \left| r_{12} \right|^2 = \left| \frac{E^-}{E^+} \right|^2$$

where r is the Fresnel reflection coefficient and is expressed as the ratio of the incident and reflected waves in the transparent first phase. The reflectivity of a three phase system (fig. 1A) is given by $R_{123} = |r_{123}|^2$ and by analogy the Fresnel reflection coefficient for a three phase system is defined as

$$r_{123} = \frac{r_{12} + r_{23}e^{-2i\beta}}{1 + r_{12}r_{23}e^{-2i\beta}}$$

where a complex quantity representing the change in phase and amplitude of the beam during one traversal of the film phase of thickness d is given by

$$\beta = \frac{2\pi \hat{n}_2 \, d \cos\Theta_2}{\lambda}$$

Since the reflectivity of a film free two phase system, R_{13}, is identical to that of a three phase system with d=0, R_{13} and R_{123} can be written as R(0) and R(d). Spectroscopic measurement of the absolute reflectivity is very difficult when the reflecting substrate surface is enclosed in an experimental cell. However, it is possible to make accurate measurements of the ratio R(d) / R(0) since various optical system errors occur as common factors and cancel. In most cases the thickness of the adsorbed layer (d) is very much smaller compared to the wave length of incident radiation. Hence, it is possible to a make a first order approxi-

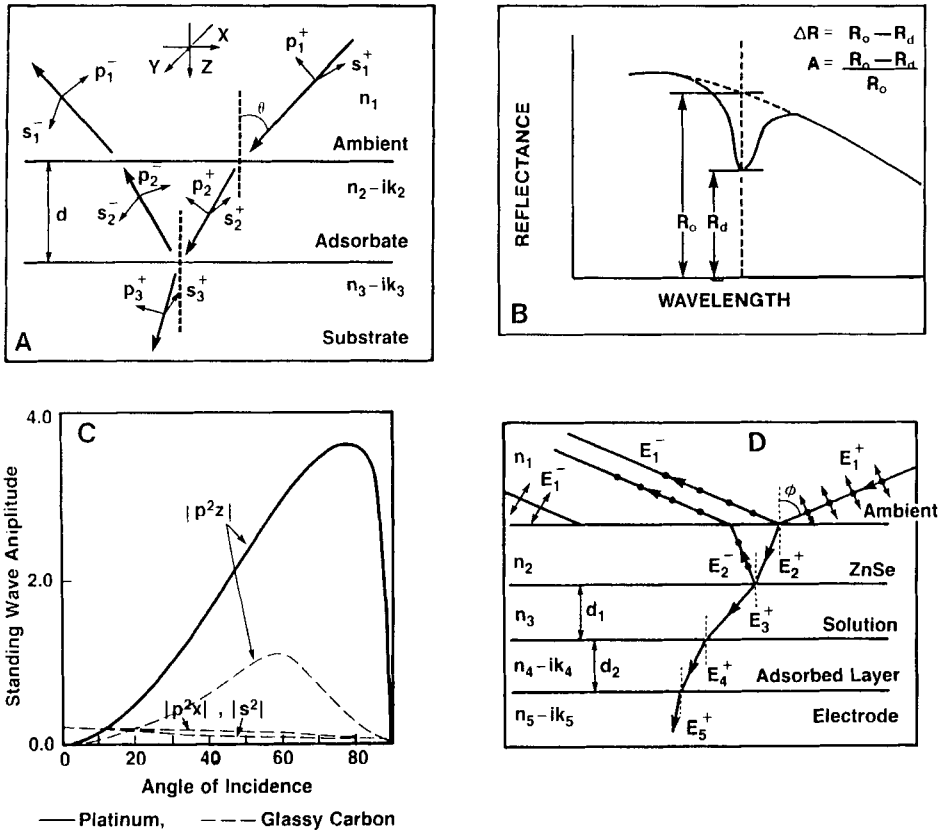

1) (A) Electric field vectors in a three phase system.

(B) Definition of absorption factor.

(C) Nature of the standing wave fields as a function of angle of incidence at a platinum and glassy carbon surface.

(D) Path of the IR beam through a thin layer cell in the presence of an adsorbed layer.

mation for the reflecivity ratio (6) and from the linear approximation theory, the reflectivity ratio for the two polarizations, "s" (perpendicular to the incident plane) and "p" (parallel to the incident plane) can be expressed as

$$\frac{Rs\,(d)}{Rs\,(0)} = 1 + \frac{8\pi d n_1 \cos\Theta_1}{\lambda}\ \mathrm{Im}\left[\frac{\mu_3\hat{\varepsilon}_2\cos^2\Theta_2 - \mu_2\hat{\varepsilon}_3\cos^2\Theta_3}{\mu_3\varepsilon_1\cos^2\Theta_1 - \mu_1\hat{\varepsilon}_3\cos^2\Theta_3}\right]$$

$$\frac{Rp\,(d)}{Rp\,(0)} = 1 + \frac{8\pi d n_1 \cos\Theta_1}{\lambda}\ \mathrm{Im}\left[\frac{\mu_2\hat{\varepsilon}_3\cos^2\Theta_2 - \mu_3\hat{\varepsilon}_2\cos^2\Theta_3}{\mu_1\hat{\varepsilon}_3\cos^2\Theta_1 - \mu_3\varepsilon_1\cos^2\Theta_3}\right]$$

where θ_1, θ_2, and θ_3 are the angles as defined in figure 1A.

n_1 is the refractive index of the first phase.

μ_j is the magnetic permeability of the media.

ε_j and ε_j are the complex and real dielectric constants of the system.

The linear approximation theory is valid for both internal and specular reflection modes and for all angles of incidence.

Actually, the reflection ratio calculated this way is not the primary quantity desired. What is really needed is a measure of the depth of an absorption band in the thin layer so that it is possible to compare the value of the reflectivity of the thin absorbing layer on a metal surface with the reflectivity of the same with no absorption in the thin layer. A convenient measure of the depth of an absorption band obtained from a reflection system is a normalized reflectivity change and is known as the absorption factor "A" (7) (fig. 1B).

$$A = \frac{\Delta R}{\bar{R}} = \frac{R(0) - R(d)}{R(0)} = 1 - \frac{R(d)}{R(0)}$$

At low frequency (infrared and microwave) the conductivity of a good

conductor approaches its dc value (8)($=10^{17}$ sec^{-1} for metals with K>10). Hence, the reflectivity of a metal in the infrared region is very close to unity since

$$R = \left[1 - \frac{2\omega}{\pi\sigma_0}\right]^{1/2}$$

A metal with high conductivity cannot support an electric field. Since the component of E that lies parallel to the surface must be the same on either side of the surface and also because the E field inside a perfect conductor must be zero, the tangential component of the E field outside the surface of a perfect conductor must also be zero. This is equivalent to saying that the E field is always perpendicular to the surface of a perfect conductor (k>10). Therefore, in addition to the infrared selection rule, the metal surface imposes the restriction that only those vibrations which have a component of their oscillating dipole moment normal to the metal surface are active in the IR (9,10). Pearce and Sheppard (11) have named this the metal surface selection rule. This sensitivity towards orientation is a very valuable feature of IR specular reflection spectroscopy. Thus the sensitivity for spectroscopic determination of a surface film on a highly reflecting metal surface is virtually nil at normal incidence and at all angles of incidence if the radiation is perpendicularly polarized (s). Vector addition of incident and reflected vectors at the surface of a metal gives rise to a standing wave and the amplitude of the standing wave for the s and p_x components exhibit a node at the surface. For instance, in the 2000cm^{-1} (5μ) spectral range, the distance between the node and adjacent antinode of the standing wave is 12500Å(7) which is much more than 2000 times the thickness of a 5Å layer of adsorbed material. Only the p_z component has an antinode at the surface and the amplitude of the standing wave increases with angle of incidence, reaches a maximum value

of about 4 times that of the incident radiation around 80° and rapidly decreases to zero at θ=90° (fig. 1C). In the case of a carbon surface however, calculations (12) show that both p and s components at the surface are non zero (fig.1C). The maximum standing wave intensity for the s component is observed at normal incidence and is only 0.2 times the incident radiation. The maximum for the p_z component occurs at 59° and is 1.2 times the incident radiation. Hence, the ideal situation for spectroscopic determination of thin films would be to use the appropriate high angle of incidence and p-polarized radiation.

EXPERIMENTAL

Fourier Transform Infrared (FT-IR) Spectrometer

The instrument used in the present studies is the Nicolet 7199 FT-IR spectrometer and its optical layout is shown in fig.2. The heart of the instrument is a Michelson interferometer which consists of a beam splitter (BS1) and a fixed (M4) and moveable mirror. Radiation from a continuum source (S1), focussed on an aperture (A1) and collimated by an off-axis spherical mirror (M2), enters the interferometer. The beamsplitter (BS1) reflects about half of the beam to the fixed mirror and transmits the other half to the moveable mirror. These two split beams are then reflected back to the beam splitter and the combined beam is then split again with about half going back to the source and the other half passing through the sample compartment to the detector (D2). When the distance from the beam splitter to the fixed and moveable mirrors are equal, that is, the optical retardation (x) between the two arms of the interferometer is zero, constructive interference occurs and the beam leaving the beam splitter has maximum intensity. When the optical retardation is not zero, the beams from the two arms of the interferometer interact destructively depending on the phase change for each wavelength. Since all wavelengths enter the interferometer, the

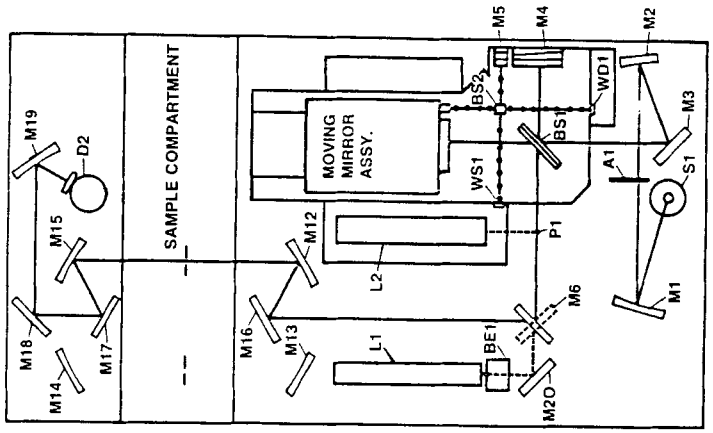

SI	-Source	M16,M17	-2-Position, Computer-Controlled Flat Mirrors
MI	-Spherical Mirror, 4.5"E.F.L.		
A1	-Aperture and Chopper	M12,M13,	
M2	-Sperical Mirror, 9.0" E.F.L.	M14,M15	-Off-Axis Parabolic Mirros,9.3" E.F.L.
M3	-Flat Mirror	M18	-Flat Mirror
BS1	-Beamsplitter and Compensator	M19	-Off-Axis Parabolic Mirror,3.5" E.F.L.
BS2	-White Light Beamsplitter	D2	-IR Detector
M4	-Fixed Mirror	L2	-Centerline Laser
M5	-White Light Mirror	L1	-Alighment Laser
P1	-Centerline Laser Prism	BE1	-Beam Expander
M6	-4-Position, Computer-Controlled Flat Mirror	M20	-Flat Mirror
		WS1	-White Light Source
		WD1	-White Light Detector

White Light Beam
Infrared Beam
Laser Beam

Nicolet 7199 Optical Layout

2) Optical layout of the Nicolet-7199 FTIR spectrometer.

interferogram consists of polychromatic radiation and for an ideal Michelson interferometer the mathematical expression for the intensity (I) at each displacement (x), is given by

$$I(x) = \int_0^{+\infty} 2I(\nu)\, R(\nu)\, T(\nu) \left\{1 + \cos\,(2\pi\nu x)\right\} d\nu$$

where ν is the wavenumber of radiation in nitrogen (in the case of the Nicolet 7199 instrument), $I(\nu)$ is the intensity of radiation for wavenumber ν and $R(\nu)$ and $T(\nu)$ are the reflectance and transmittance of the beam splitter at wavenumber ν. For a 100% efficient beam splitter $R(\nu) = T(\nu) = 0.5$, so that

$$I(x) = \tfrac{1}{2} \int_0^{+\infty} I(\nu) \left\{1 + \text{Cos } (2\pi\nu x)\right\} d\nu$$

The AC component of the interferogram is called the interferogram function $F(x)$ and is the quantity measured by the instrument.

$$F(x) = I(x) - I(\infty) = \int_0^{+\infty} A(\nu) \text{ Cos } (2\pi\nu x) \quad d\nu$$

where $A(\nu) = 2I(\nu) R(\nu) T(\nu) = I(\infty)$

since at $x = \infty$ the $\text{Cos}(2\pi\nu x)$ term averages to zero

A single beam spectrum is obtained from the interferogram by performing a Fourier transformation on $F(x)$ to give

$$A(\nu) = \int_{-\infty}^{+\infty} F(x) \text{ Cos } (2\pi\nu x) \quad dx$$

and since $F(x)$ is an even function, symmetric about $x = 0$, we have

$$A(\nu) = 2 \int_0^{+\infty} F(x) \text{ Cos } (2\pi\nu x) \quad dx$$

Thus a transmittance spectrum is obtained by ratioing the sample spectrum to the instrument background.

In practice, the interferogram cannot be measured to a retardation of 0 to ∞ and the effect of using a finite retardation causes the spectrum

to have a finite resolution. This effect and others are described in detail by Griffiths (13).

Although there are several advantages (13) of using a FT-IR spectrometer over a grating instrument, the main advantages can be summarized as follows:

1). The Fellget or multiplex advantage arises from the fact that the FT-IR spectrometer examines the entire spectrum at the same time whereas the grating instrument measures only one spectral element at a time. Since the S/N ratio improves as the square root of observation time of each resolution element, the FT-IR system improves the S/N ratio by a factor of $(S/\Delta\nu)^{\frac{1}{2}}$ where S is a spectral region between ν_1 and ν_2 with resolution $\Delta\nu$.

2). Jacquinot's or throughput advantage results from the loss of energy in the dispersive system due to the gratings and slits. These losses do not occur with an FT-IR instrument which does not contain these elements.

3). The Conne or frequency advantage comes from the fact that the frequencies of an FT-IR instrument are internally calibrated by a laser whereas conventional instruments exhibit drifts when changes in alignment occur. This advantage is particularly useful for the co-addition of interferograms to signal average since the frequency accuracy is an absolute requirement in this case.

The throughput advantage is very important for the in situ characterization of electrochemical reactions, since almost all solvents have high absorption in the infrared and a large portion of the energy is lost in

the process. Also, the multiplex advantage permits the recording of the complete spectrum of species in a short time which is particularly useful for detecting and monitoring the presence of short-lived intermediates during electrochemical reactions.

Specular Reflectance Assembly

The reflection attachment used was a modified version of the apparatus described by Harrick (14) (fig. 3A). The converging beam from the interferometer was reflected by a plane mirror M1 to the plane mirror M2 of a retroreflector placed such that any desired angle of incidence could be obtained at the cell window. The cell window and the electrode formed the second reflecting element of the retroreflector. The two reflectors were placed at an angle of 97.5° with respect to each other in order to accommodate the beam focus of the Nicolet FT-IR cavity. After transmission through the window, the beam was reflected by the electrode, followed by another spherical mirror M3 and directed to the focussing optics of the detector through a plane mirror M4.
As described earlier (fig. 1C), only p-polarized radiation is capable of interacting with surface dipoles. Hence, for surface work with metal electrodes, the Brewster angle was chosen at the window. This was because, at the Brewster angle the reflected light is linearly polarized with the electric vector perpendicular to the incident plane (s-polarized) and 100% of the p-polarized radiation is transmitted at the first interface.(15)

The infrared radiation was filtered by a silicon Brewster angle polarizer (Harrick Scientific) mounted before the detector so that only p-polarized radiation reached the detector and the s-polarized component, which does not contain much information and would decrease the dynamic range of the A

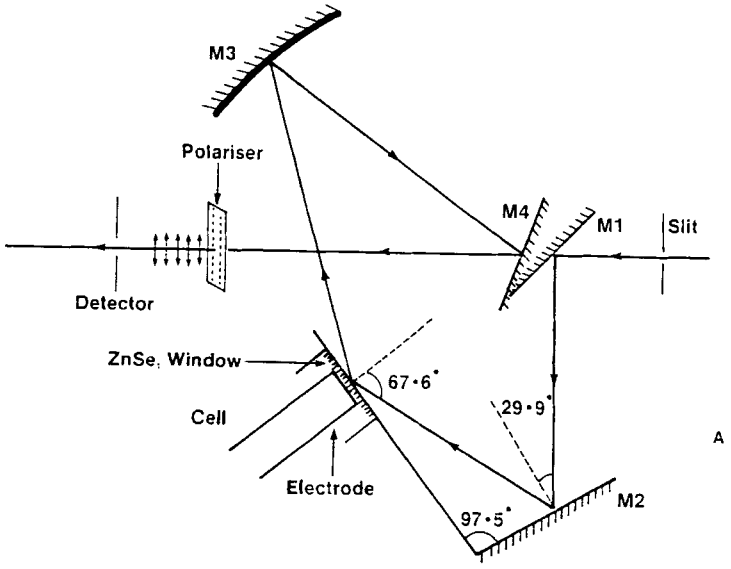

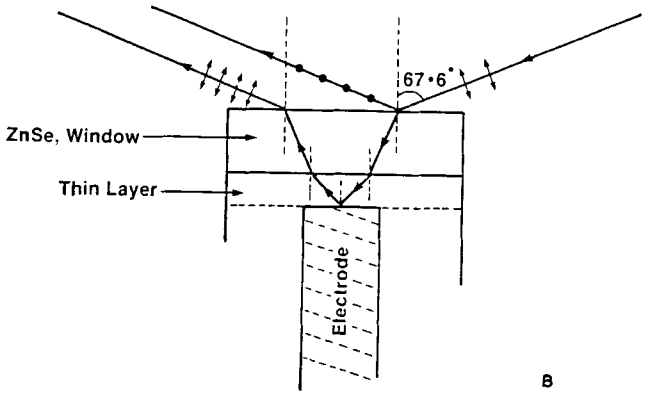

Path of an IR beam through the cell

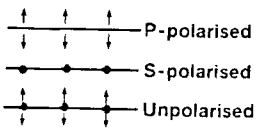

3) (A) Optical layout of a specular reflection system.

(B) Path of the IR beam through the cell at Brewster angle.

to D converter, was eliminated. For the characterization of bulk species, any angle of incidence at the window can be used since the randomly oriented species in solution will interact with both polarizations.

The entire reflectance accessary was mounted on a x-y-z positioner and the cell was fixed in place with the help of a separate x-y-z positioner.

Cell Design

For spectroscopic studies of species in strongly absorbing solvents, particularly water, the main requirement in the design of the cell is a small path length for the beam. This is to ensure that sufficient IR energy is left after passing twice through the solution layer (fig.3B) enabling thereby the detection of a very small change in absorbance due to the electroactive species in the presence of a large excess of solvent molecules.

The design of a three electrode spectroelectrochemical cell is shown in fig. 4. The working electrode consists of a 1cm diameter flat disc of the desired electrode material, sealed at the end of a stainless steel rod. The whole rod is press fitted in a teflon tube so that only the front surface is in contact with the solution. The electrodes prepared this way are very stable both mechanically and chemically in contrast to electrodes prepared using epoxy adhesives because of the possibility of the epoxy dissolving in the solvent and contaminating the test solution. The electrode surface was polished with 0.05μ γ alumina and was cleaned ultrasonically. A Luggin capillary probe for the reference electrode was placed close to the working electrode. A platinum ring co-axial with the working electrode served as a counter electrode. The total cell volume was about 10 ml. The optical window was mounted at the end of the

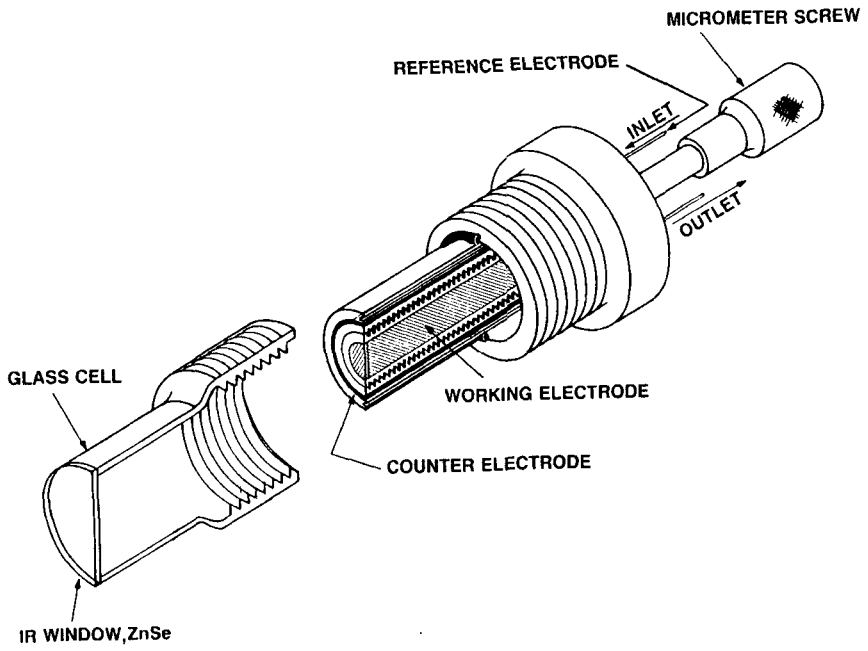

4) Variable pathlength spectroelectrochemical cell.

cell in such a way that the electrode surface and the window, when brought close, were in perfect contact with each other, thus maintaining a uniform solution thickness across the entire electrode surface.

The choice of window material basically depends on the frequency range of interest and the type of solvent used. As discussed earlier, the sensitivity of the method increases with a high angle of incidence (fig. 1B). Since the Brewster angle and hence the angle of incidence at the electrode increases with the refractive index, it is essential to choose a window material with the highest refractive index. Considering all the parameters, ZnSe (70% transmission, n = 2.5) is a good choice for the mid IR.

The cell designed as described works as a variable path length cell. For surface work the electrode surface was kept very close to the window so that a very thin layer (ca. 1μ) configuration existed at the electrode surface and the contribution of the solution species in the observed spectra was minimized.

For investigating the solution species, the electrode surface was moved back with an attached micrometer screw so that a larger volume of the solution could be sampled. The solution thickness could be precisely controlled with the micrometer screw or could be determined spectroscopically using the following expression (in the absence of any electric field)

$$d = \frac{10^4 A}{2\varepsilon C} \text{Cos} \left\{ \text{Sin}^{-1} n_1 / n_3 \text{Sin} \phi \right\}$$

where d is the solution thickness in microns, A is the integrated absorbance of a particular infrared band, ε is the molar extinction coefficient, C is the molar concentration and ϕ is the angle of incidence (fig. 1D). For a pure solvent εc can be replaced by K, the extinction coefficient.

The cell described herein acts as a multi-layer system. However, since the first two phases are always the same and the optical properties constant, in the simplest approximation, the electrode-electrolyte interfacial region can be described as a three phase stratified system with plane parallel boundaries formed when a homogeneous, isotropic thin film of uniform thickness is generated on the electrode surface. It can thus be represented by Fig. 1A, and the reflection theory described earlier can be applied.

In the present system about 49% of the incident s-polarized radiation was lost at the ZnSe surface due to reflection and 100% of the p-polarized and the remaining 51% of the s-polarized radiation were transmitted at the Brewster angle. The angle at the electrode surface was about 45°. Under this condition the standing wave amplitudes for platinum and carbon would respectively be 2·0 and 1·1 times the incident radiation.

Data Collection and Calculation of $\Delta R/R$

Potential step input waveforms were provided by a Model 173 potentiostat and Model 175 function generator (both PARC). Synchronization between the application of the potential step and the beginning of the data collection was controlled by a Hewlett-Packard 9816 computer, although it can also be controlled with the help of an external trigger available in the Nicolet 7199 FTIR spectrometer. There are two basic timing sequences that can be used depending upon whether the electrode solution interface is reversible or irreversible with respect to the modulating electrode potential. In the case of a reversible system, four co-added interferograms were collected after the steady state condition had been reached at each of the two set potential limits ($E_{ref.}$ and $E_{sam.}$) and stored separately (fig. 5). The cycle was repeated "n" times until two sets of "4n" co-added interferograms of the required S/N was obtained (typically n equals 20 and 25 in non-aqueous and aqueous media respectively). In the case of solution species such as radical ion intermediates, a time interval was introduced between each cycle. Typically the electrode was pulsed for 4 seconds at E_{sample} and 4 interferograms collected. Then with the potential at $E_{reference}$ an interval of 10 seconds (or as required) was allowed before the 4 interferograms were collected so as to exclude the interference due to the presence of radicals (if any).

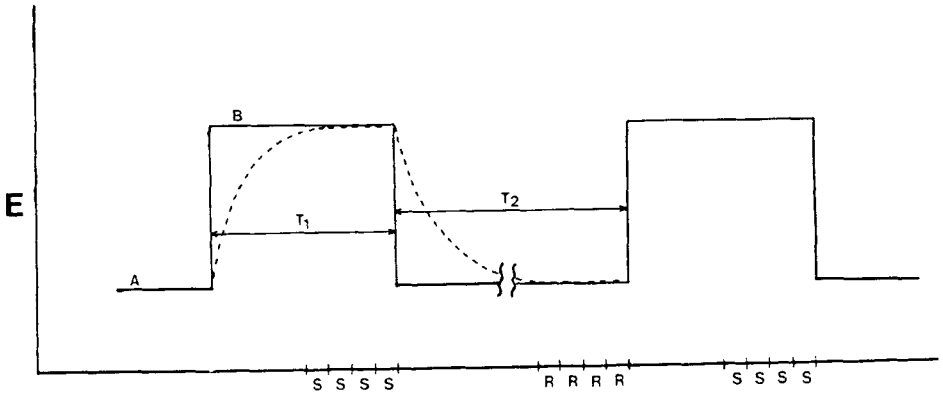

5) Synchronization of the potential step and the beginning of data collection. S and R represent a single scan at sample (B) and reference (A) potentials.

For an irreversible system, instead of pulsing, the potential of the electrode was held at particular reference and sample potentials and about 100 co-added interferograms were collected at each potential. Interferograms were Fourier transformed to give single beam spectra.

The change in infrared absorption as a function of potential is represented by the absorption factor (as discussed earlier)

$$A = \frac{R(o) - R(d)}{R(o)}$$

In the present case

$$A = \frac{R(ref.) - R(sam.)}{R(ref.)}$$

where $R_{ref.}$ and $R_{sam.}$ are the reflectivities at reference and sample potentials.

In terms of electric field strength

$$A = \frac{|\bar{E}_{ref}|^2 - |\bar{E}_{sam}|^2}{|\bar{E}_{ref}|^2}$$

where $\bar{E}_{ref}$ and $\bar{E}_{sam}$ (fig. 1A) represents the electric field strength of the reflected radiation at reference and sample potentials.

Since I (intensity) is proportional to the mean square electric field strength, the abosrption factor can be represented as

$$A = \frac{I_{ref.} - I_{sam.}}{I_{ref.}} = \frac{\Delta R}{R} = \frac{\Delta I}{I}$$

a quantity which can be very easily computed in an FTIR instrument by digital substraction of two individual single beam spectra and ratioing them to the reference spectrum

The final spectrum obtained this way is a normalized difference spectrum and only represents the changes between the two states. In the present case therefore all peaks extending to positive values of $\Delta R/R$ will signify increased absorption at that wave length at sample potential relative to the reference potential and vice versa.

If there is no change in the infrared spectrum due to change in potential, the difference spectrum will be a straight line at zero value of $\Delta R/R$.

The possible origin of various features which may arise from spectral substraction are presented in fig. 6.

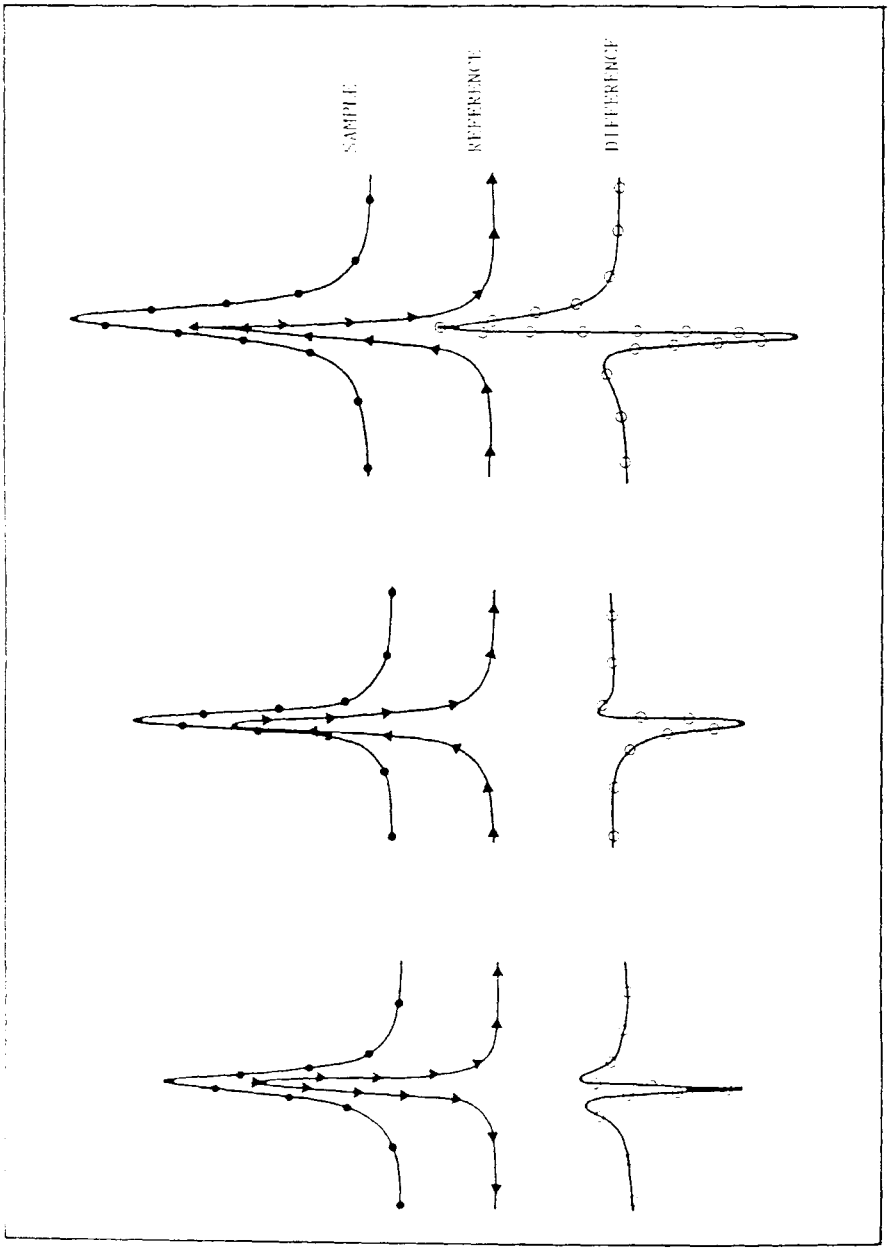

6) Effect of spectral substraction on the band shape.

Materials and Reagents

Acetonitrile (Burdick and Jackson Lab, HPLC grade) was dried over alumina before use. For studies in aqueous media, triple distilled deionized water was used. Tetra-n-butylammonium tetrafluoroborate (TBAF) (Southwestern Analytical Chemical, Inc.) was used as a supporting electrolyte in acetonitrile solutions. Benzophenone, N,N,N´,N´-tetramethyl p-phenylene diamine (TMPD) and N,N,N´,N´-tetramethyl benzidine (TMBD) were obtained from Aldrich Chemical Company and were used without further purification. Various substituted anilines were synthesized (16,17). Tetracyanoethylene (TCNE) (Aldrich Chemical Co.) was vacuum sublimed to give white crystals, m.p. 201-2°C.

All potentials in non-aqueous and aqueous solutions were measured against $Ag/AgNO_3$ (IBM) and SCE (IBM) reference electrodes respectively.

A glassy carbon disc (1 cm diameter) (Tokai Carbon Co. Ltd., Japan) was used as the carbon electrode.

APPLICATION OF THE TECHNIQUE

Various electrochemical systems covering a wide range of molecules have been studied in aqueous and acetonitrile media using platinum and carbon electrodes.

Studies on Platinum Electrode

1. Ferrocyanide/ferricyanide system from aqueous media

The redox couple $Fe(CN)_6^{-3}/Fe(CN)_6^{-4}$ is probably one of the most extensively studied systems in homogeneous and heterogeneous electron transfer investigations. However, little is still known about the interaction between ferro or ferricyanide with the working electrode although recent data (3,18,19) indicate that these interactions may lead

to adsorption. In the present work therefore, the system has been spectroscopically investigated in aqueous sulfate solution. All studies were done with 10mM $K_4Fe(CN)_6$ in 0.5M aqueous K_2SO_4 solution.

The difference spectra, as a function of anodic potential, obtained using the pulse (potential modulalen) technique, is shown in Figure 7. The reference potential in each case was -0.2V and each spectrum is an average of 100 scans. The band at 2040 cm^{-1} (directed upward) is due to the depletion of ferrocyanide at positive potentials, whereas the band at 2114 cm^{-1} (directed downward) represents the formation of ferricyanide. The 2040 cm^{-1} and 2114 cm^{-1} bands are due to the F_{1u} mode of the C≡N stretching vibration of ferro and ferricyanide molecules respectively. The intensity of both these bands was found to decrease with increasing anodic limits and with increasing number of scans at a particular potential limit (20). These observations are indicative of electrochemical irreversibility in the system. This is further evident from the single beam spectra (fig. 8). Initially at the reference potential (fig. 8A) only one band at 2040 cm^{-1} corresponding to the νC≡N of ferrocyanide is observed. At positive potential however (fig. 8B) two bands at 2098 cm^{-1} and 2114 cm^{-1} are observed, out of which, as indicated earlier, the band at 2114 cm^{-1} corresponds to the νC≡N of ferricyanide. On reversal of the potential to -0.2V (fig. 8C) the band at 2114 cm^{-1} disappears whereas the one at 2040 cm^{-1} reappears with substantially reduced intensity. This indicates that the concentration of ferrocyanide species and hence also of the ferricyanide species, decreases with successive pulses. The 2098 cm^{-1} band on the other hand remains unchanged and was found to be present even after flushing the thin layer with fresh solution. This band is obviously due to some irreversible reaction and has been accordingly assigned to the νC≡N of species adsorbed on the surface of the platinum electrode. Although the

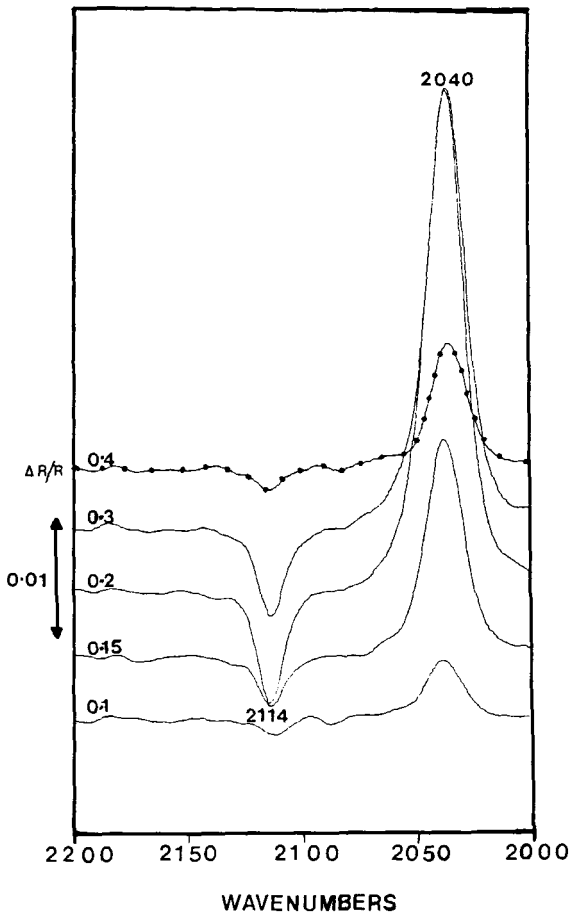

7) Normalized difference spectra of aqueous ferrocyanide solution as a function of anodic potential.

presence of adsorbed spcies is indicated by the single beam spectra, the difference spectra obtained by the potential modulation technique gives no evidence of adsorption. It is apparent therefore that this technique is limited to reversible systems only.

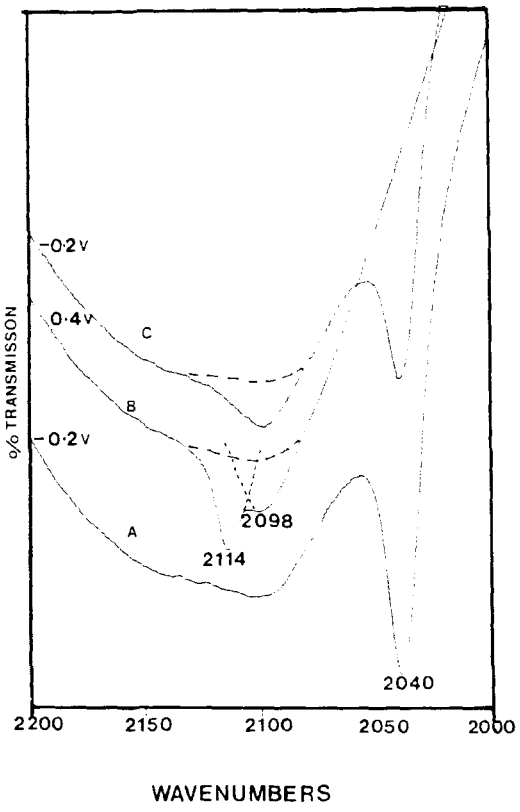

8) Potential dependence of the single beam spectra of aqueous ferrocyanide solution.

To overcome this limitation a different method of data collection was used in which 100 scans were taken at the reference and each of the sample potentials. The normalized difference spectra (fig. 9) obtained this way clearly reveal the presence of the band at 2098 cm^{-1}. The intensity of the band increases with increasing positive potential whereas the intensities of the 2040 cm^{-1} and 2114 cm^{-1} bands reach a maximum at +0.3V and then decrease. The adsorbed species were found to

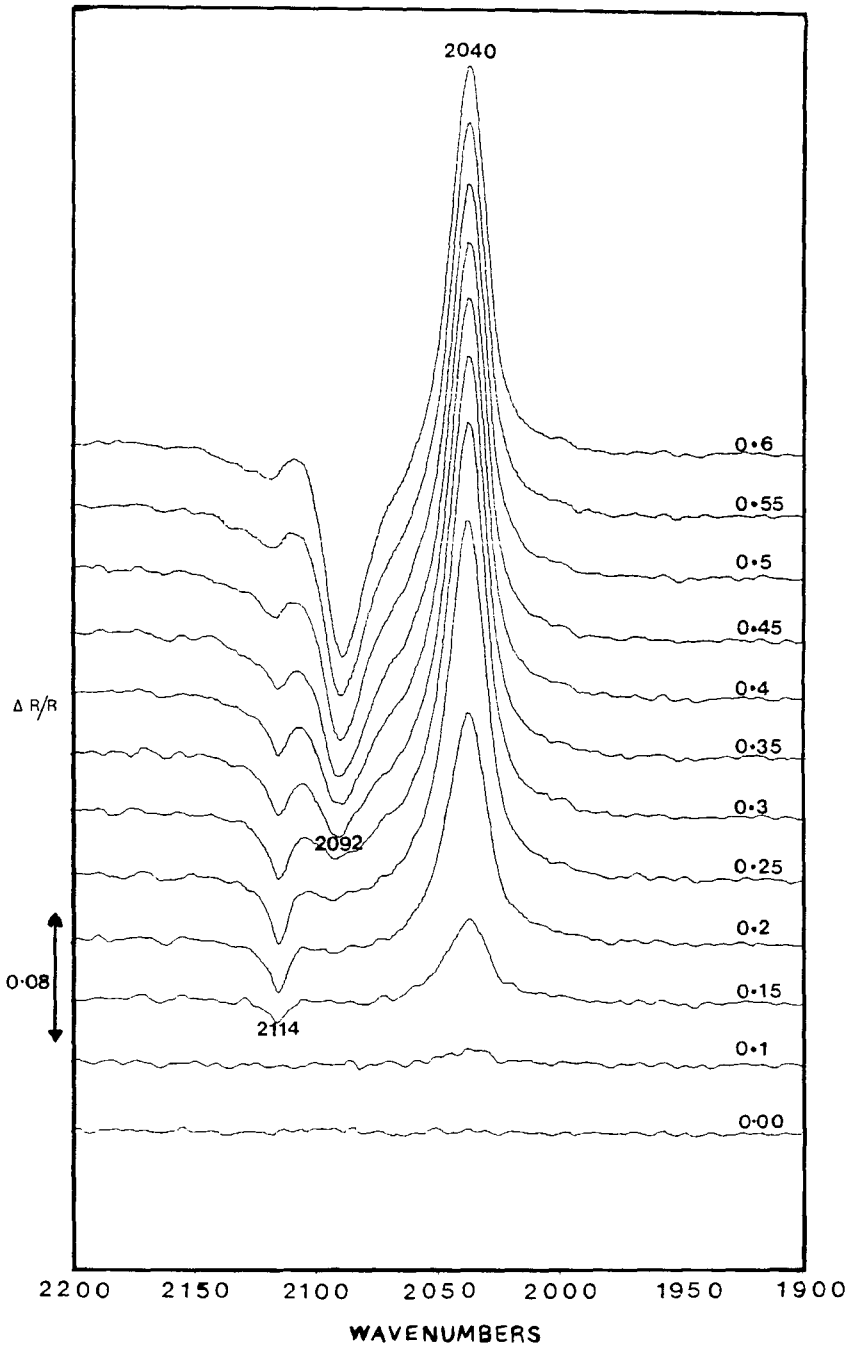

9) Normalized difference spectra of aqueous ferrocyanide solution as a function of anodic potential.

be stable even after removing the electrode from the solution as evident from the fact that the ex-situ infrared reflection spectrum shows the same band. Consequently, the adsorbed species was characterized by ex-situ x-ray photoelectron spectroscopy and far IR studies (20). It was found from the binding energies of iron and nitrogen and from the iron to nitrogen ratio that the adsorbed species is prussian blue. The presence of two photoelectron peaks for nitrogen and their ratio suggests that the adsorbed species are bound to the platinum surface through nitrogen. This explains the positive shift of the $\nu_{C\equiv N}$ stretching frequency upon adsorption ($\nu_{C\equiv N}$ for prussian blue is 2087 cm^{-1}). It is suggested therefore that the ferrocyanide initially adsorbs on the electrode and at high positive potential acts as a precursor for the formation of prussian blue.

2. Benzophenone anion radical from acetonitrile solution

The infrared difference spectrum of a 5mM solution of benzophenone in acetonitrile, in the interfacial region, is shown in figure 10A. The cyclic voltammogram of the solution showed that benzophenone can be reduced to its anion radical (which is blue in color) at -2.5V and hence the electrode potential was stepped from -1.0V to -2.8V.

As stated earlier, peaks going upwards represent the vibrational frequencies of benzophenone whereas those pointing downward correspond to the vibrational frequencies of species formed at -2.8V. The extinction coefficient of both the reactant and product are comparable in this case. The vibrational frequencies of the anion radical have previously been assigned (21) and are in good agreement with observed frequencies. Also, ESR studies show that the odd electron density is primarily localized on the carbonyl group and consequently $\nu_{C=O}$ decreases by ca. 270 cm^{-1} on going from the neutral ketone to its anion

radical (21). Frequencies of the other modes, however, decrease by about 30 cm^{-1}. The broad band at 1060 cm^{-1} is due to the BF_4^- species and the disappearance of the band at -2.8V is a good indication that the solution layer is very thin and that one is actually looking at the interfacial region. The band at 1660 cm^{-1} has been assigned to the νC=O of benzophenone and the νC=O of the radical, expected around 1396 cm^{-1}, is seen as a band of medium intensity. The bands at 2116 cm^{-1} and 1519 cm^{-1} have not been reported previously and have also not been observed in the case of the benzophenone anion radical generated in THF (21). A comparison of figures 10A and 11 shows that these bands at 2116 cm^{-1} and 1519 cm^{-1} are seen only in the interfacial region and disappear upon increasing the solution thickness to more than 1μ (fig. 11). The position of the 2116 cm^{-1} band indicates that it is due to a nitrile stretching vibration, and since no such band is expected for either benzophenone or its anion radical, it would appear that this band results from the interaction of the radical with the solvent.

The electro reduction of carbonyl compounds, PhCOR (R=Me, Ph, H), in acetonitrile is known to give significant amounts of α-β unsaturated nitriles due to the reaction of the electrogenerated cyanomethyl anion ($-CH_2CN$) with the carbonyl compound (22, 23). The 2116 cm^{-1} and 1519 cm^{-1} bands have therefore been assigned to the νC≡N and νC=C of the α-β unsaturated nitrile ($(Ph)_2C=CHCN$). It is likely that this non electrochemical step in the reaction takes place more effectively near the electrode surface than in the bulk owing to the higher concentration of base in the vicinity of the electrode. This probably explains the presence of the 2116 cm^{-1} and 1519 cm^{-1} bands in the interfacial region. Whether these species are adsorbed on the electrode is being investigated (24).

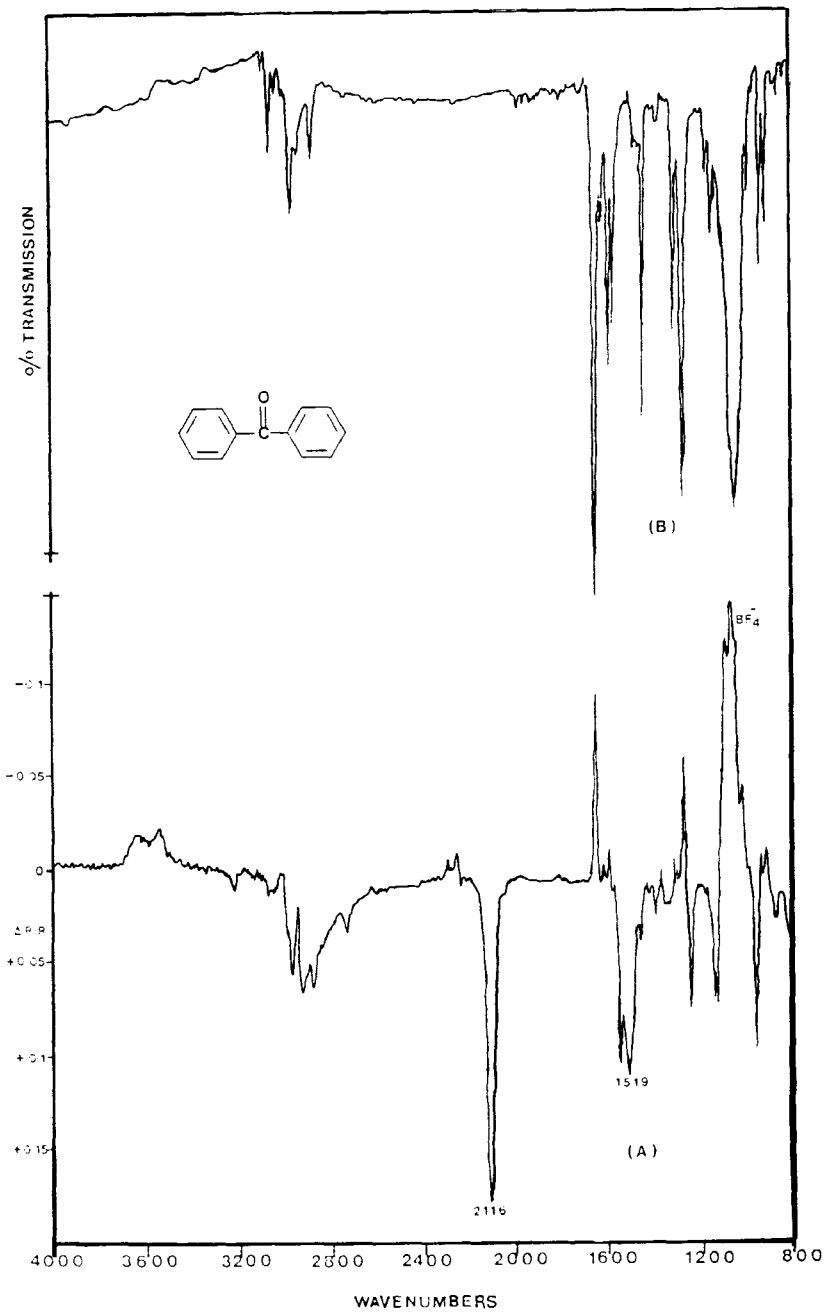

10) (A) Normalized difference spectrum of benzophenone in acetonitrile solution between -1.0V and -2.8V through ca. 1μ solution.

(B) Transmission spectrum of benzophenone from acetonitrile solution (solvent substracted).

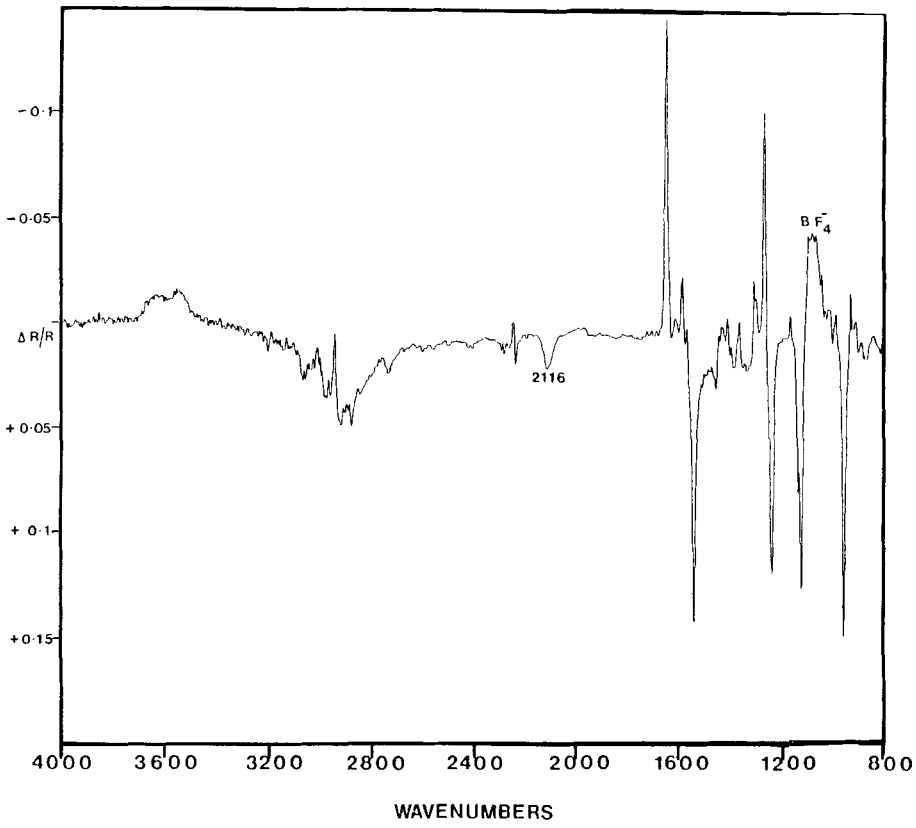

11) Normalized difference spectra of benzophenone in acetonitrile solution between -1.0V and -2.8V through solution thickness of more than 1μ.

3. Substituted anilines from acetonitrile media

In the present work, the oxidation of 2,6-di-tert-butyl-4-R anilines (R=Phenyl, p-methylphenyl, p-methoxyphenyl and p-ethoxyphenyl) in acetonitrile solution has been spectroscopically investigated. In all cases 5mM solution of anilines were used. The first oxidation wave (ca. 0.6V) of these anilines have been electrochemically investigated (16)

and is known to be a reversible one electron transfer process leading to the formation of the cation radical. Due to the short lifetime of the radicals the potential modulation technique was used for data collection. Figure 12A represents the typical difference spectrum obtained between 0.0V and 0.8V through a 1μ solution. The transmission spectrum of the parent compound (fig. 12B) in solution shows that the symmetric and asymmetric N-H stretching frequencies occur at 3440 cm^{-1} and 3520 cm^{-1}. The corresponding N-H frequencies for the radicals occur at much lower wave numbers (fig. 13) with the extent of lowering increasing with decreasing electronegativity of R. This decrease in the N-H stretching frequency indicates that an electron from the lone pair of nitrogen is removed during radical formation. This is also evident from the larger downshift of the symmetric N-H stretch compared to the asymmetric stretch of the radicals since the lone pair on nitrogen is involved in the symmetric stretching mode (25).

In addition to the shift in the N-H stretching frequency, the $\nu_{C=C}$ of the aromatic ring system of the radicals were, in general, found to shift towards higher frequency by about 50 cm^{-1} (fig. 14). This suggests that the odd electron is not localized on nitrogen but is also delocalized over the ring system and the increase in the $\nu_{C=C}$ vibration is due to the quinoid structure of the ring. An interesting feature observed in the 1600 cm^{-1} region for all the compounds in the interfacial region, was the presence of two bands around 1640 and 1580 cm^{-1}. The band at 1640 cm^{-1} has been assigned to the $\nu_{C=C}$ vibration of the radical in solution (26). The 1580 cm^{-1} band on the other hand was not observed when the solution thickness was increased and may therefore be due to the effect of the electric field on the molecules very close to the surface. The origin of the band is under investigation (27).

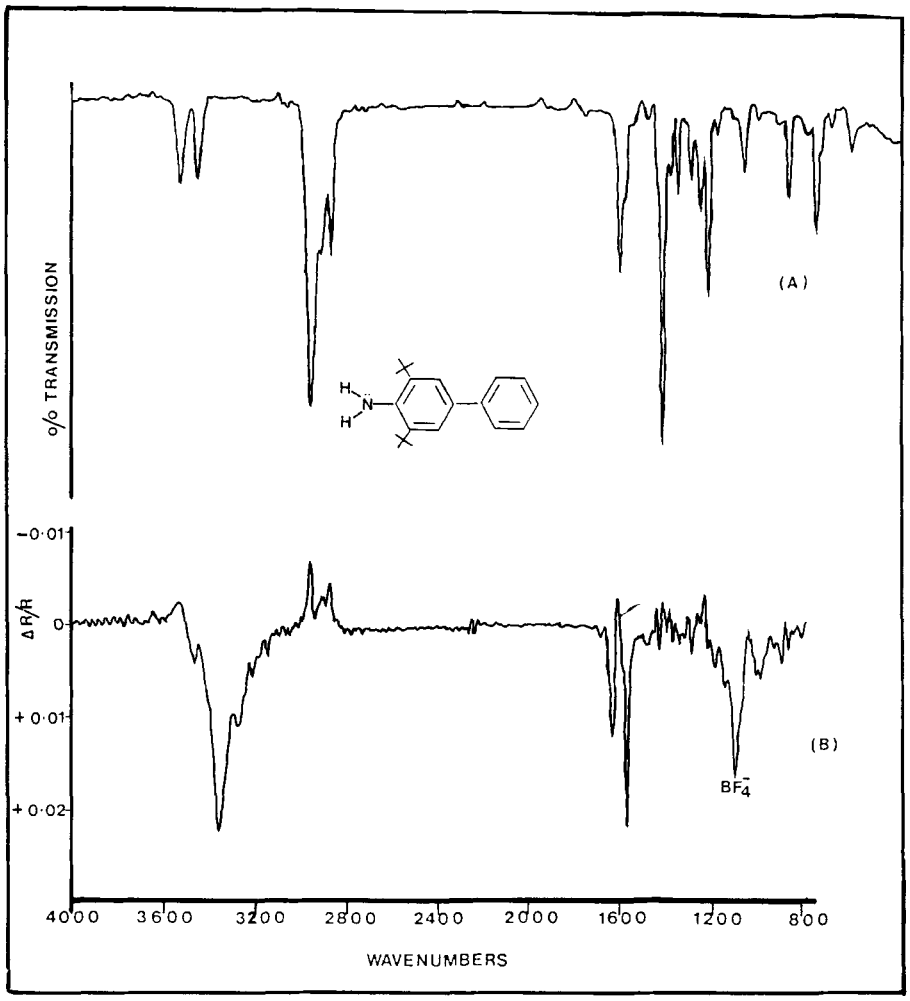

12) (A) Transmission spectrum of 2,6,di-tert-butyl-p-phenyl aniline in acetonitrile (solvent subtracted).

(B) Normalized difference spectrum of 2.6-di-tert-butyl-p-phenyl aniline in acetonitrile solution between 0.0V and +0.8V.

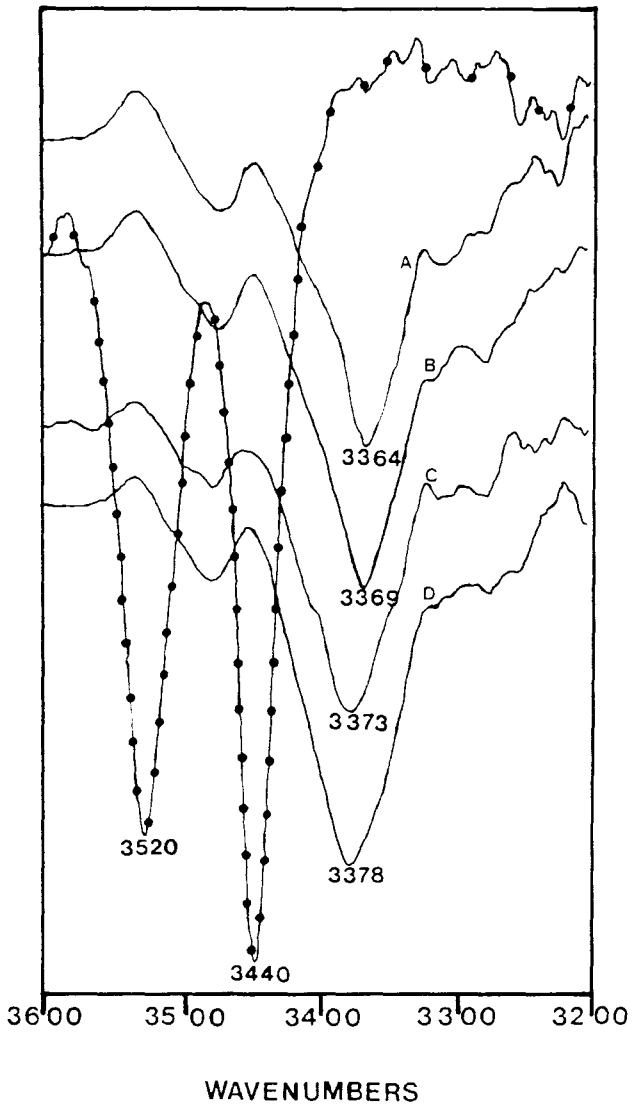

13) N-H stretching vibration of 2,6-di-tert-butyl-4-R-anilines (---) and their radical cations (——). (A) R=Phenyl, (B) R=p-methyl phenyl, (C) R=p-methoxy phenyl and (D) R=p-ethoxyphenyl.

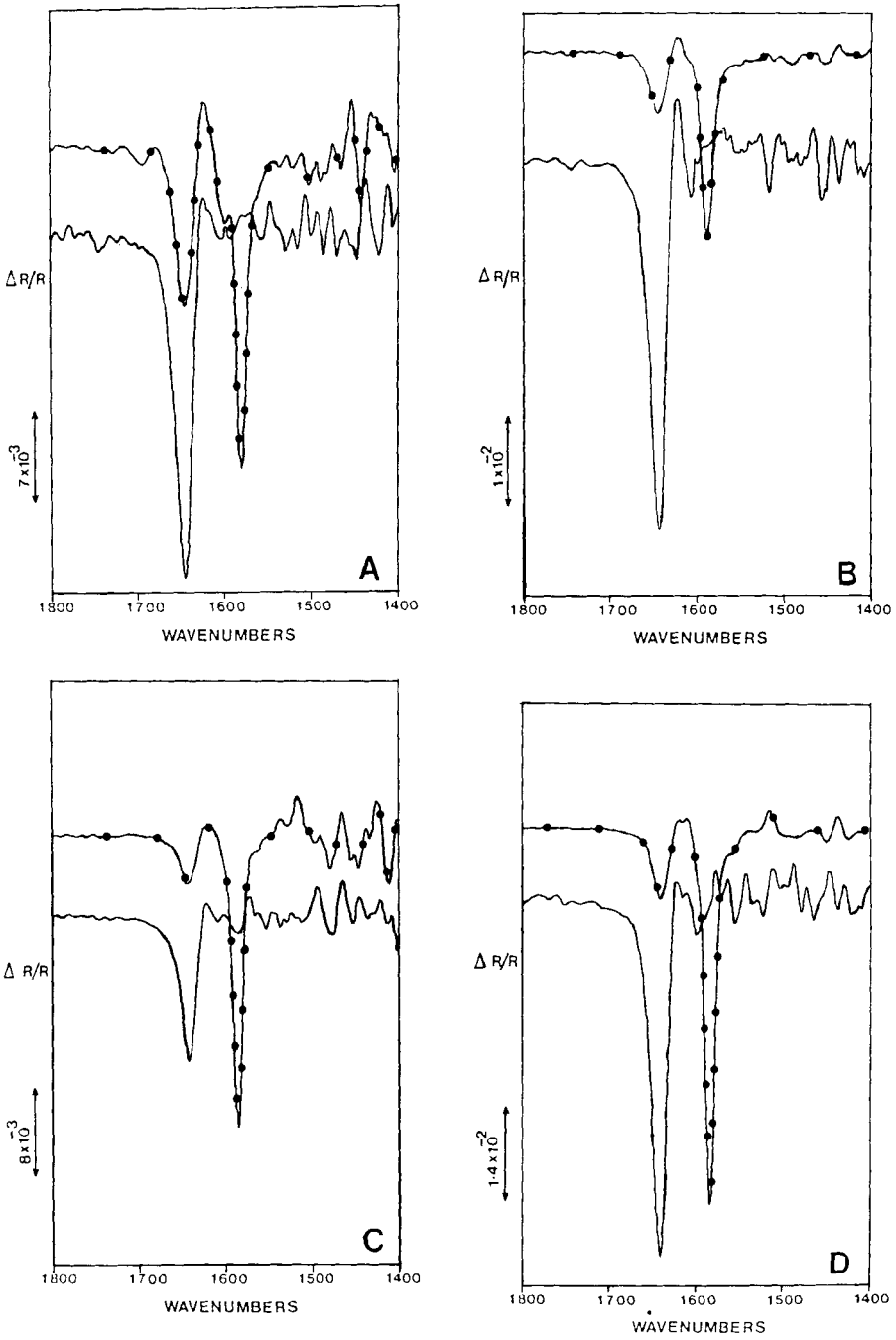

14) Effect of solution thickness on the difference spectrum of electrogenerated radical cations.

—●— solution layer ca. 1μ

—— solution layer > 1 μ

4. TMPD and TMBD in acetonitrile media

Figures 15 and 16 represent the difference spectra of TMPD and TMBD from acetonitrile solution obtained by the potential modulation technique. One electron oxidation of TMPD (0.05V) and TMBD (0.34V) leads to the formation of the radical cations and their vibrational frequencies are in good agreement with literature values (2). Owing to the intense visible color of the TMPD radical cation, it has been studied by resonance Raman spectroelectrochemistry but no such studies using in situ FTIR spectroscopy have so far been reported.

Studies on Carbon Electrode

All in situ IR and FTIR studies reported in the literature so far have been done with optically nonabsorbing electrodes made of shiny metals. However, since shiny metals are rarely used as commercial electrodes, the sensitivity of the present technique towards industrial conditions, has been investigated using a glassy carbon electrode (a typical industrial electrode).

1. Adsorption of phosphate ion from aqueous solution

In the present case adsorption of phosphate was studied from aqueous buffer of pH=8.0. Figure 17 (A and B) represent the single beam IR spectra of phosphate solution at potentials of +1.0V and -1.0V and figure 17C represents their normalized difference spectrum. At positive potential, the spectrum shows two bands around 1000 cm^{-1} and 1080 cm^{-1}, whereas only one band around 1000 cm^{-1} is observed at negative potential. Free phosphate ion which belongs to the point group Td, has two IR active fundamentals of F_2 symmetry (ν_3 and ν_4) (28, 29). The band at 1000 cm^{-1} corresponds to the ν_3 vibration of the P-O asymmetric stretch of free phosphate ion in solution. The ν_4 vibration expected around 500 cm^{-1} was not observed due to the high absorption of water in that region.

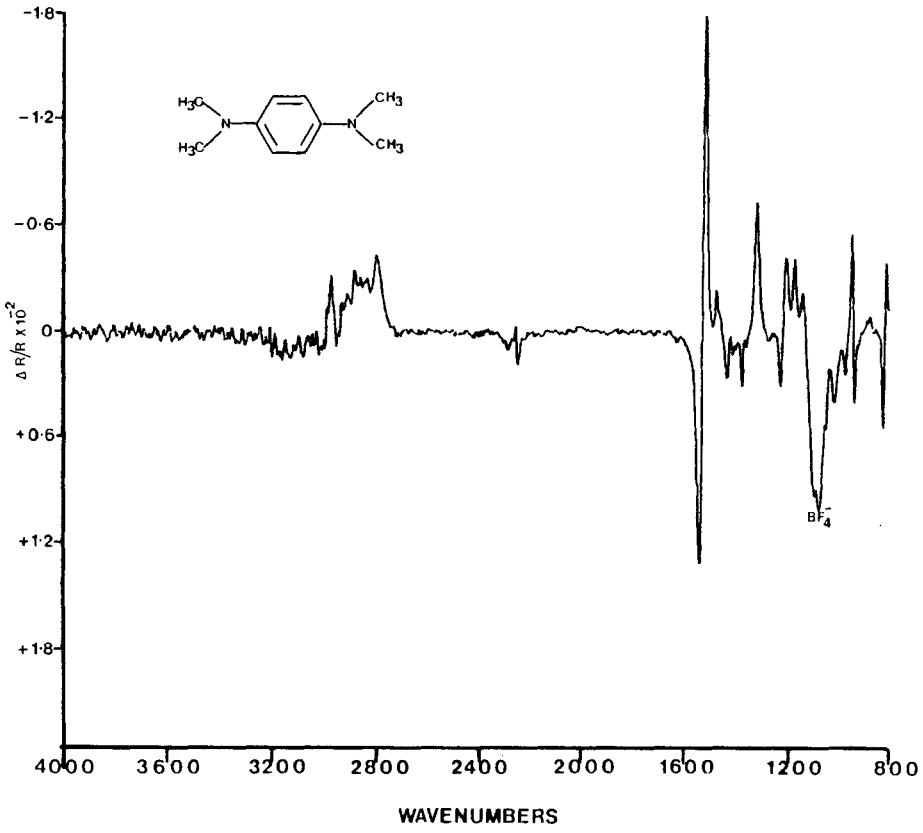

15) Normalized difference spectrum of TMPD in acetonitrile solution between -0.3V and +0.3V.

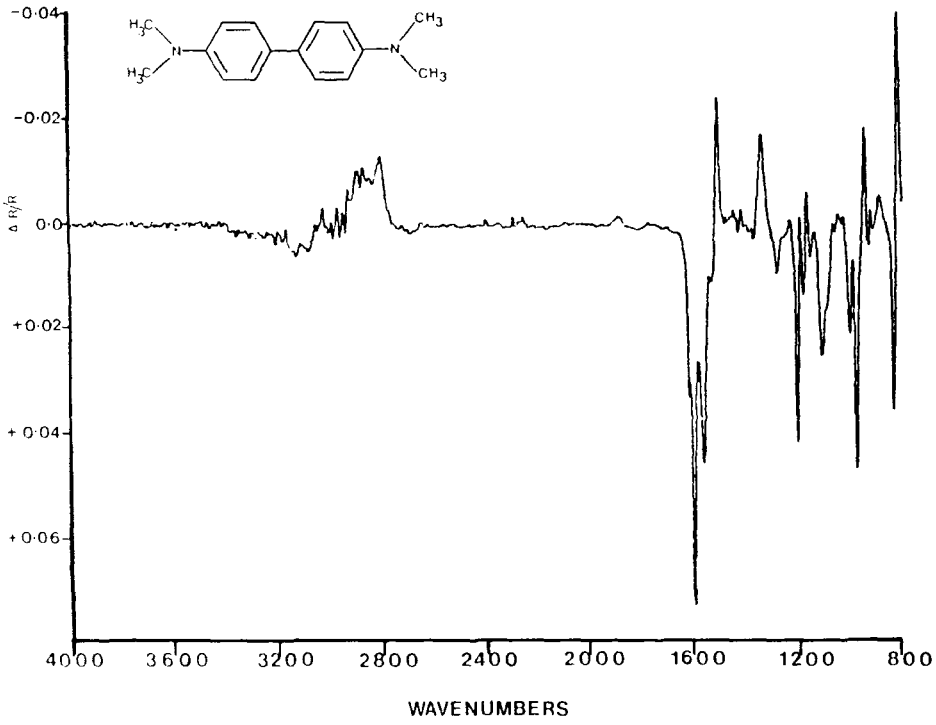

16) Normalized difference spectrum of TMBD in acetonitrile solution between -0.2V and +0.5V.

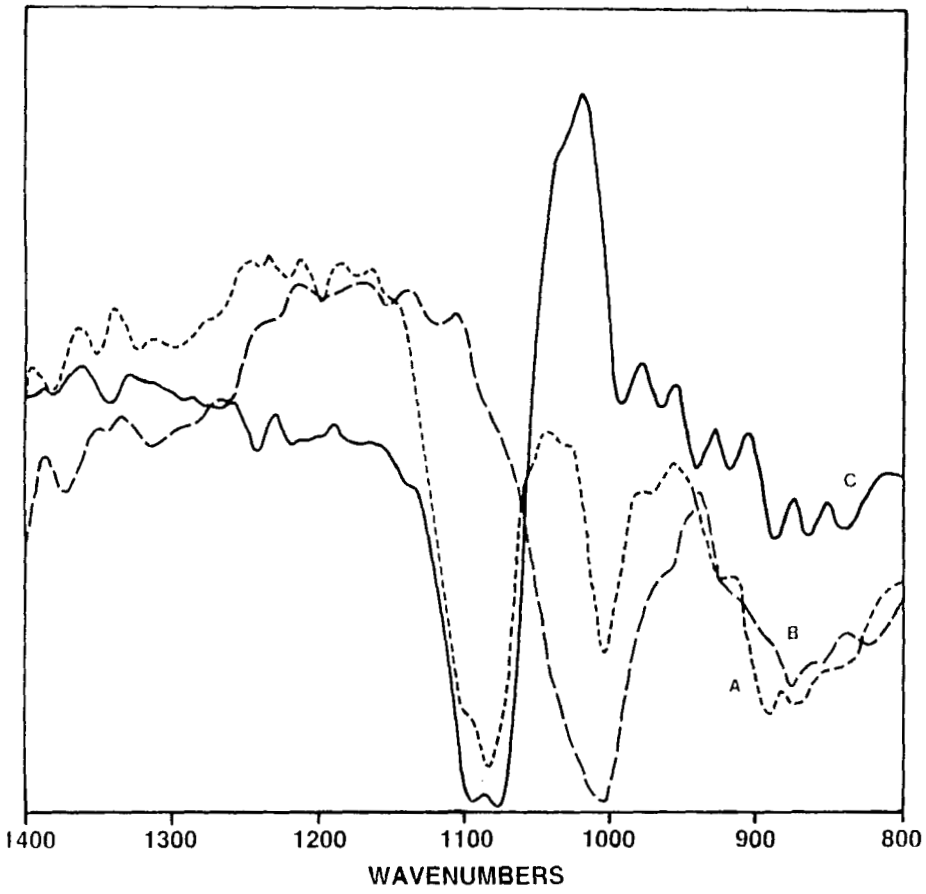

17) Spectra of aqueous phosphate solution at carbon electrode through ca. 1μ solution.

(A) Single beam spectra at +1.0V

(B) Single beam spectra at -1.0V

(C) Difference spectrum between -1.0V and +1.0V

The band at 1080 cm^{-1}, whose intensity was found to increase with anodic potential (29), has on the otherhand, been assigned to the ν_3 vibration of adsorbed phosphate. The shift of the ν_3 band to higher frequency, at positivle potential, without any measurable splitting of the band, seems to indicate that the tetrahedral symmetry of phosphate is essentially retained and the adsorbed molecule has a dipole component perpendicular to the electrode surface.

2. TCNE anion radical from acetonitrile solution

The presence of oxygen functional groups on carbon has long been postulated and it is believed that these groups strongly affect the adsorption behaviour on carbon. In order to investigate the presence and influence of such groups, the adsorption behaviour of the highly reactive tetracyanoethylene (TCNE) anion radical on carbon, has been investigated. Such studies on a platinum electrode have been reported earlier (4).

The cyclic voltammogram of TCNE solution in acetonitrile shows two reduction waves at -0.05V and -1.3V corresponding to the formation of the anion and the dianion respectively (30). Figure 18 represents the typical difference spectrum of a 2 mM solution of TCNE in acetonitrile containing 0.1M TBA, between +0.5V and -0.5V. The intense upward directing peak at 1060 cm^{-1} corresponds to the increase in the concentration of BF_4^- species in the interfacial region at positive potential. The bands at 2150 cm^{-1} and 2190 cm^{-1} have been assigned to the $\nu C{\equiv}N$ of the anion radical in solution (4). The extinction coefficient of $\nu C{\equiv}N$ of TCNE (2220 cm^{-1}) is much less than that of the radical and is hence not observed in the spectrum. Figure 19 represents the C≡N stretching region of the spectra obtained between the reference potential (+0.5V) and various sample potentials. At lower sample potentials (-0.4

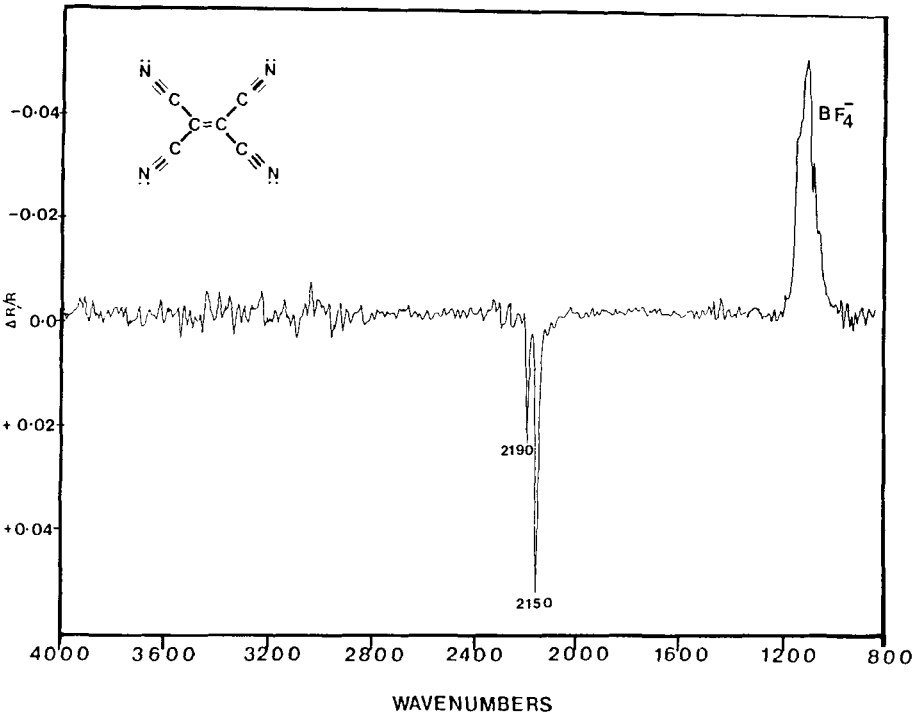

18) Normalized difference spectrum of TCNE in acetonitrile solution between +0.5V and -0.5V.

and -0.7V) only two bands are observed at 2150 and 2190 cm^{-1} corresponding to the anion radical in solution. At more negative potential (-1.0V) however, bands due to the anion radical disappear and new bands appear at 2198, 2165 and 2125 cm^{-1} along with a weak band at 2075 cm^{-1}. The 2125 cm^{-1} and 2165 cm^{-1} bands have been assigned to the $\nu C{\equiv}N$ of the dianion (31). However, extending the sample potential just past the second reduction wave results in an additional band at 1680 cm^{-1} and a much more intense band at 2075 cm^{-1} (fig. 20A). It is evident from figure 20A and 20B that

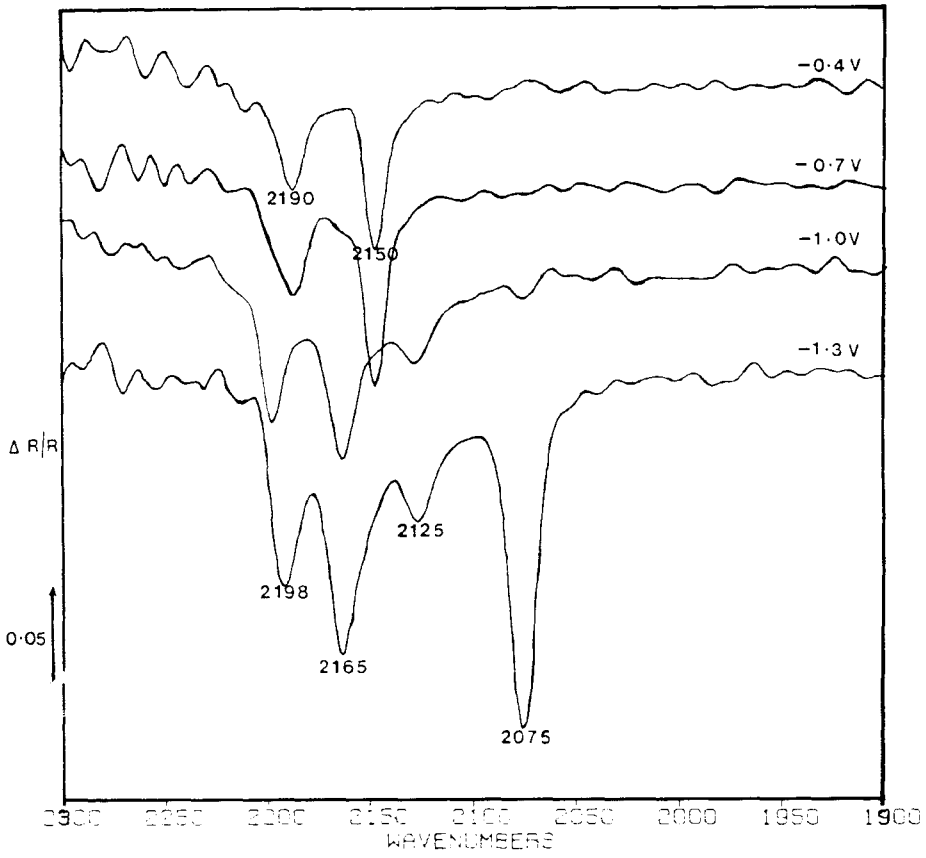

19) Normalized difference spectrum of TCNE in acetonitrile solution as a function of sample potential.

the 1680 cm^{-1}, 2075 cm^{-1} and 2198 cm^{-1} bands are only observed in the interfacial region since their intensities decrease as the solution thickness increases and are hence assigned to surface species. Similar experiments carried out on a platinum electrode however showed only one surface band at 2075 cm^{-1} (30). It appears therefore that in the case of carbon, there are more than one kind of surface species. The 2075 cm^{-1}

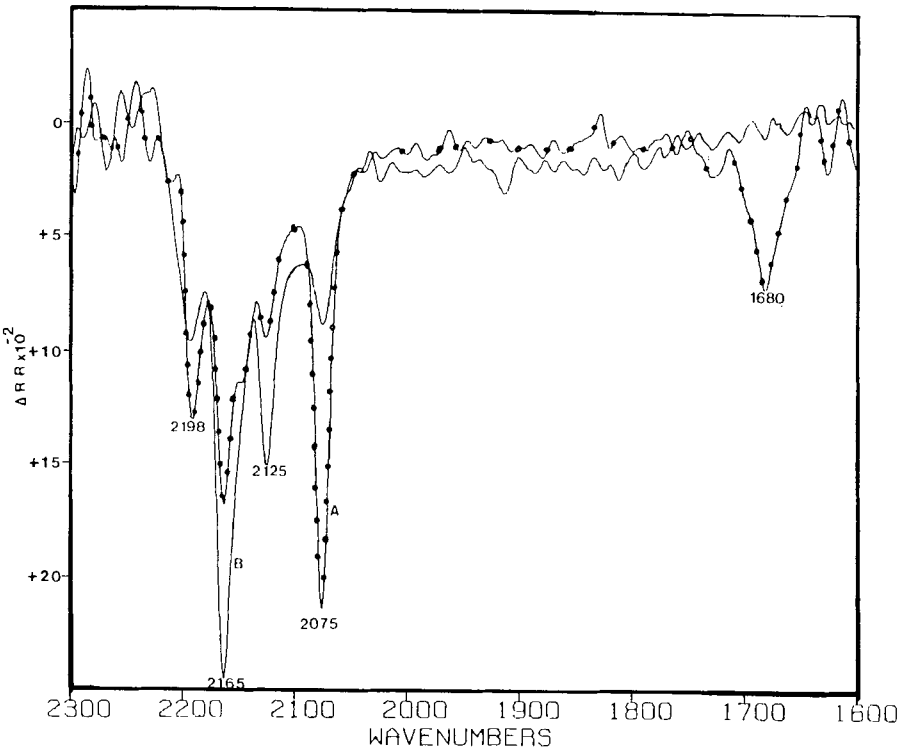

20) Normalized difference spectra of TCNE solution between +0.5V and -1.3V

(A) solution layer ca. 1μ

(B) solution layer > 1μ

band has been assigned to the adsorbed dianion since the lowest unoccupied orbital of the TCNE molecule is antibonding with respect to carbon and nitrogen and $\nu_{C\equiv N}$ is therefore expected to decrease on adsorption through the transfer of an electron from the electrode to the radical (32). The

origin of the bands at 2198 cm^{-1} and 1680 cm^{-1} is less obvious since no bands are expected around the 1600 cm^{-1} region for either TCNE or its anion radical.

It is known (33) that the TCNE anion radical invariably forms a pentacyanopropenide (PCP) ion in solution whose $\nu C{\equiv}N$ is in the region of 2198 cm^{-1}. It is also known that the TCNE anion adsorbed from solution on alumina forms the tricyanovinyl alcoholate ion (TVA) by the interaction of the anion radical with the surface hydroxyl group of alumina (34, 35). The $\nu C{\equiv}N$ and $\nu C{=}O$ of the TVA ion are expected around 2198 cm^{-1} and 1660 cm^{-1} respectively (36). It would appear therefore that the TCNE anion radical reacts with surface hydroxyl groups on carbon to form the TVA ion on the surface of carbon. Moreover the 20 cm^{-1} shift of the $\nu C{=}O$ vibration suggests that the TVA ion is bound to the carbon surface through oxygen. The 2198 cm^{-1} band could be due to both PCP and TVA as they lie in the same region. PCP may be formed at the surface but probably diffuses out into the bulk whereas TVA is adsorbed on the electrode. The present results indicate therefore that unlike the case of platinum, the TCNE anions adsorb on carbon both as the dianion and the TVA ion. These results therefore provide for the first time in situ infrared evidence for the presence of oxygen containing functional groups on carbon and their influence on the adsorption process. Electrochemical evidence for the presence of such groups on carbon in acetonitrile media have also been obtained in our laboratory (37).

CONCLUSION

In the present work a diverse selection of problems have been investigated and it is evident that FTIR spectroscopy can be very effectively used for the in situ characterization of electrochemical processes and for identifying the nature and structure of adsorbed species

and reaction intermediates. This technique is also important in the wider context of surface science since the control of the electrode potential enables the electronic properties of the substrate surface to be modified thus opening up new possibilities for studying the adsorbate-adsorbent interaction. Moreover, although FTIR spectroscopy has recently been successfully used for the study of electrochemical systems involving shiny metal electrodes, the present studies have demonstrated for the first time the applicability of the technique for monitoring adsorbed species and reaction intermediates also on commercial electrodes such as carbon even through aqueous media. In view of the tremendous potential of this technique however, there is an obvious need for more theoretical work to provide a deeper understanding of the infrared spectra of adsorbed species particularly under the influence of an electric field.

REFERENCES

1. J.D.E. McIntyre, "Advances in Electrochemistry and Electrochemical Engineering," R.H. Muller, Ed. (John Wiley Int., New York, N.Y. 1973), Vol. 9, p. 66.

2. R.E. Hester, "Advances in Infrared and Raman Spectroscopy," R.J.H. Clark and R.E. Hester Ed. (Heyden and Son Inc., Philadelphia, PA 1978) Vol. 4, p. 1.

3. S. Pons, M. Datta, J.F. McAleer and A.S. Hinman, J. Electronal. Chem., 160, 369 (1984).

4. S. Pons, S.B. Khoo, A. Bewick, M. Datta, J.J. Smith, and G. Zachman, J. Phys. Chem., 88, 3575 (1984).

5. A. Bewick, K. Kunimatsu, B.S. Pons and J.W. Russel, J. Electroanal. Chem., 160, 47 (1984).

6. J.D.E. McIntyre and D.E. Aspens, Surf. Sci., 24, 417 (1971).

7. R.G. Greenler, J. Chem. Phys., 44, 310 (1966).

8. M.E. Bennett, J.M. Bennett, E.J. Ashley and R.J. Motyka, Phys. Rev., 165, 755 (1966).

9. N.V. Richardson, Surf. Sci., 87, 622 (1979).

10. R.G. Greenler, Surf. Sci., 118, 415 (1982).

11. H.A. Pearce and N. Sheppard, Surf. Sci., 59, 205 (1976).

12. M. Datta, J.J. Freeman and R.E.W. Jansson, in preparation.

13. P.R. Griffiths, "Chemical Infrared Fourier Transform Spectroscopy," (John Wiley and Sons, New York, 1975).

14. N.J. Harrick, Appl. Optics., 10, 2344 (1971).

15. G.R. Fowles, "Introduction to Modern Optics," (Holt, Rinehart and Winston Inc., New York, 1975) p. 47.

16. B. Speiser, A. Rieker and S. Pons, J. Electroanal. Chem., 147, 205 (1983).

17. B. Speiser, A. Rieker and S. Pons, J. Electroanal. Chem., 159, 63 (1983).

18. A. Wieckowski and M. Szklarczyk, J. Electroanal. Chem., 142, 157 (1982).

19. J. Kwiatek, T. Jendral and Z. Galus, J. Electroanal. Chem., 145, 163 (1983).

20. M. Datta and A. Datta, submitted for publication.

21. I. Juchnovski, Ts. Kolev and I. Rashkov, Spectroscopy Lett., 18, 171 (1985).

22. G.W. Gokel, S.A. Dibiase and B.A. Lipisko, Tetrahedron Letters, 39, 3495 (1976).

23. A.J. Bellamy, J.B. Kerr, C.J. McGreger and I.S. MacKirdy, J.C.S. Perkin II, 161 (1982).

24. M. Datta, in preparation.

25. P.J. Krueger, Can. J. Chem., 40, 2300 (1962).

26. M. Datta and B. Speiser , in preparation.

27. M. Datta, in preparation.

28. K. Nakamoto, "Infrared and Raman Spectra of Inorganic and Co-ordination Compounds," (J. Wiley and Sons, New York, NY, 1978) p. 142.

29. M. Datta, J.J. Freeman and R.E.W. Jansson, Spectroscopy Lett., 18, 273 (1985).

30. M. Datta, R.E.W. Jansson and J.J. freeman, Spectroscopy Lett., 19, 129 (1986)

31. M. Datta, "FTIR reflection absorption technique applied for the characterization of electroactive species," paper presented at the 5th International Conference on Fourier and Computerized Infrared Spectroscopy, Ottawa, Canada, June 24-28, 1985.

32. J.C. Moore, D. Smith, Y. Youhne and J.P. Devlin, J. Phys. Chem., 75, 325 (1971).

33. M.J. Shine and R.D. Goodin, J. Org. Chem., 35, 949 (1976).

34. U. Mazur and K.W. Hipps, J. Phys. Chem., 88, 1555 (1984).

35. U. Mazur and K.W. Hipps, J. Phys. Chem., 86, 5105 (1982).

36. U. Mazur and K.W. Hipps, J. Phys. Chem., 86, 2854 (1982).

37. F.E. Woodard, private communication.

Date Received: 04/29/86
Date Accepted: 07/03/86